PHYSICAL REVIEW D VOLUME 35, NUMBER 12 15 JUNE 1987

Neutrino oscillations and the solar-neutrino problem

A. Dar, A. Mann, Y. Melina, and D. Zajfman
Department of Physics and Space Research Institute Technion, Israel Institute of Technology, Haifa, Israel
(Received 7 November 1986)

The values of neutrino masses and mixing angles which are required by the Mikheyev-Smirnov-Wolfenstein (MSW) solution to the solar-neutrino problem are found from analytic solutions to the neutrino propagation equations in the Sun. They coincide with those obtained through extensive numerical computations by Rosen and Gelb. They divide into three classes of oscillation parameters that can solve the solar-neutrino problem. The gallium solar-neutrino experiment will be able to test only two alternatives. However, the third alternative yields sizable oscillations of atmospheric neutrinos in Earth which can be detected by the massive deep-underground proton-decay detectors and neutrino telescopes. Finally, some solutions yield a sizable amplification of neutrino oscillations in Earth which change both the flavor and the spectrum of solar neutrinos that reach terrestrial detectors at night. The day-night modulation of the flux of solar neutrinos perhaps can be used to establish their solar origin in the radiochemical detectors and the MSW solution to the solar-neutrino problem.

I. INTRODUCTION

If the neutrinos, which are produced in weak interactions, are not stationary states of the Hamiltonian, they will evolve in time to produce neutrino oscillations,[1] which is the analog in the leptonic sector of the K^0-$\overline{K}^0$ oscillations. Such oscillations *in vacuo* were first considered by Pontecorvo[2] who showed that the probability of oscillations in a vacuum is measurable if the neutrinos are not degenerate. A few years later when Bahcall and Davis[3] reported that the rate of ^{37}Ar production by the reaction $\nu_e + {}^{37}\mathrm{Cl} \rightarrow e^- + {}^{37}\mathrm{Ar}$ in the chlorine solar-neutrino experiment of Davis is much smaller than that expected of solar neutrinos, several authors[1,4] proposed that it may be due to neutrino oscillations: If ν_e's, which are produced by the thermonuclear reactions in the core of the Sun (with $E_\nu \lesssim 14$ MeV), oscillate and reach Earth as ν_μ's (or ν_τ's), they escape detection in the chlorine solar-neutrino experiment because their energy ($E_\nu \leq 14$ MeV) is below the threshold energy for the reactions $\nu_l + {}^{37}\mathrm{Cl} \rightarrow l^- + {}^{37}\mathrm{Ar}$, $l = \mu, \tau$.

The experimental results of Davis and his collaborators[5] indicate that a complete mixing of the three neutrino flavors would be required to bring theory into agreement with experiment.[6] However, neutrino oscillations have been searched extensively during the past few years and no evidence for oscillations with large mixing angles has been found.[7] But, since terrestrial measurements can measure only oscillation lengths, which are either smaller or comparable to the diameter of Earth,[1,8] while the oscillation length of solar neutrinos may be comparable to the distance to the Sun, it may be impossible for terrestrial measurements to verify the neutrino-oscillation solution with a large mixing to the solar-neutrino puzzle.

Recently, Mikheyev and Smirnov[9] have discovered that even a very small mixing angle, which yields a very small $\nu_e \rightarrow \nu_\mu$ oscillation amplitude *in vacuo* can cause an almost complete conversion of the ν_e's produced by the thermonuclear reactions in the core of the Sun into ν_μ's before they emerge from the Sun. Their discovery is based on a very interesting 1978 paper by Wolfenstein, where he showed that even a small mixing angle can lead to a complete conversion of ν_e's into ν_μ's (or ν_τ's) in matter, due to the difference between the forward-scattering amplitudes (off electrons) of ν_e's and of the other neutrinos in matter analogous to the regeneration of K_S from a K_L beam passing through matter. However, Wolfenstein has demonstrated[10] this resonance conversion only for neutrinos, which cross a slab of a *constant electron density equal to the resonant density,* and whose thickness is a half-integer product of the oscillation length in matter which depends both on the mixing angle and oscillation length in free space, and on the electron density. Because of these very restrictive conditions, Wolfenstein's discovery was not considered relevant to the solar-neutrino problem, until Mikheyev and Smirnov discovered by numerical integration of the neutrino propagation equations in the Sun that a resonance conversion of solar ν_e's into ν_μ's can take place in the Sun[9] and may explain the mystery of the missing solar neutrinos.[3,4,11] The Mikheyev-Smirnov-Wolfenstein (MSW) solution[9,10] to the solar-neutrino problem has been reexamined recently by Rosen and Gelb[12] and by Bethe.[13] These authors have tried to develop a qualitative understanding of neutrino masses and mixing angles, which are required by the MSW solution.

In particular, after very elaborate and extensive computations Rosen and Gelb found that there are two classes of oscillation parameters that can solve the solar-neutrino problem. One class corresponds to the solution found by Bethe,[12] which does not affect the flux of solar ν_e's from the *pp* reaction and consequently has only a slight effect on the expected results of the ^{71}Ga solar-neutrino experiments. The second class suppresses completely the ν_e flux from the *pp* reactions and reduces strongly the ^{71}Ge production in ^{71}Ga.

In view of the important implications of the MSW solution of the solar-neutrino problem (the possible discovery of finite neutrino masses and mixing angles and the removal of a major shadow cast over the theory of energy production in stars and stellar evolution for the past 15 years) and in view of the fact that there seems to be some differences between the results and conclusions of Mikheyev and Smironov,[9] those of Rosen and Gelb[12] and those of Bethe,[13] we have investigated independently the phenomenon of neutrino oscillations in the Sun and whether or not the MSW solution can be tested on Earth. For that purpose we have developed simple numerical and analytical methods for solving the neutrino propagation equations in matter. In particular we found closed-form solutions of the propagation equations in the Sun. We used them to derive simple closed-form expressions for the probability of solar neutrinos to emerge from the Sun as ν_μ's and for the neutrino masses and mixing angles that can solve the solar-neutrino problem. We have verified the analytic expressions by comparing them with the results of detailed numerical integrations. Generally our results and conclusions support those obtained by Rosen and Gelb.[12]

Our final conclusions are as follows. Neutrino oscillations in the Sun can be responsible for the solar-neutrino problem only if nature has selected one of three alternative combinations of neutrino masses and mixing angles. The gallium solar-neutrino experiments will be able to test two alternatives. However, the third alternative yields sizable oscillations of atomspheric neutrinos in Earth, which can be detected by the massive underground proton-decay detectors and neutrino telescopes.

Our paper is organized as follows. In Sec. II we discuss analytic solutions to the neutrino propagation equation in a medium of constant electron density, which exhibit the Wolfenstein resonance phenomenon. In Sec. III we present a simple numerical scheme, which is very useful for numerical solutions of the neutrino propagation equations in matter whose density changes with position, and for testing analytic solutions. In Sec. IV we derive analytic solutions of the neutrino propagation equations in the Sun and we use them to obtain simple closed-form expressions for the probability of the solar neutrinos to reach Earth and retain their original electron flavor. In Sec. V we demonstrate the accuracy of these expressions and use them to determine the ranges of neutrino masses and mixing angles, which can solve the solar-neutrino problem. In Sec. VI we discuss possible tests of the MSW solution to the solar-neutrino problem, employing either atmospheric neutrinos and the deep-underground massive proton-decay detectors as neutrino telescopes, looking for matter amplification of neutrinos oscillation in Earth, or solar-neutrino detectors for searching a day-night difference in the solar-neutrino flux which reaches the underground detectors. Final remarks and conclusions are drawn in Sec. VII.

II. NEUTRINO OSCILLATIONS IN A MEDIUM OF CONSTANT DENSITY

The time evolution of a wave packet describing the propagation of a highly relativistic particle of mass m and momentum k ($\hbar=c=1$) with a refraction index n is given by[14]

$$\left[\frac{d\psi}{dt}\right]_{\rm med}=\left[\frac{d\psi}{dt}\right]_{\rm free}+\left[\left[\frac{\partial\psi}{\partial x}\right]_{\rm med}-\left[\frac{\partial\psi}{\partial x}\right]_{\rm free}\right]\frac{\partial x}{\partial t}\,, \tag{1}$$

where

$$\partial x/\partial t\simeq 1,\ \ (\partial\psi/\partial x)_{\rm free}=ik\psi\,,$$

$$(\partial\psi/\partial x)_{\rm med}\simeq ikn\psi\,,$$

and

$$(d\psi/dt)_{\rm free}\simeq -i(m^2/2k)\psi\,.$$

The index of refraction n depends on N_s the density of scatterers per unit volume in the medium and on $f(0)$, the forward c.m. scattering amplitude from these particles:

$$n-1=(2\pi N_s/k^2)f(0),\ \ \text{where } (d\sigma/d\Omega)_{\rm c.m.}=|f(0)|^2\,. \tag{2}$$

Consider now the propagation of neutrinos in matter, and for simplicity assume that there are only two neutrino flavors, ν_e and ν_μ, and that the refraction index is diagonal in the neutrino flavor. If ν_e and ν_μ are not mass eigenstates of the free Hamiltonian, but a linear combination of the mass eigenstates ν_1 and ν_2 with masses m_1 and m_2, respectively,

$$\begin{bmatrix}\nu_e\\ \nu_\mu\end{bmatrix}=\begin{bmatrix}\cos\theta & \sin\theta\\ -\sin\theta & \cos\theta\end{bmatrix}\begin{bmatrix}\nu_1\\ \nu_2\end{bmatrix}\equiv U\begin{bmatrix}\nu_1\\ \nu_2\end{bmatrix}, \tag{3}$$

then the propagation of ν_e and ν_μ in matter, except for a common phase factor of no physical significance, is described by

$$\frac{d}{dx}\begin{bmatrix}\nu_e\\ \nu_\mu\end{bmatrix}\simeq\frac{d}{dt}\begin{bmatrix}\nu_e\\ \nu_\mu\end{bmatrix}=\frac{i\pi}{l_v}(\alpha\sigma_1+\gamma\sigma_3)\begin{bmatrix}\nu_e\\ \nu_\mu\end{bmatrix}, \tag{4}$$

where

$$\alpha\equiv\sin 2\theta,\ \ \gamma\equiv l_v/l-\cos 2\theta\,, \tag{4a}$$

$$l_v(\text{cm})\equiv 4\pi k/\Delta m^2$$
$$=2.47\times 10^2 E_\nu(\text{MeV})/\Delta m^2(\text{eV}^2)\,, \tag{4b}$$

$$l(\text{cm})\equiv 2\pi/k(n_{\nu_e}-n_{\nu_\mu})$$
$$=\sqrt{2}\,\pi/G_F N_e=\frac{1.63\times 10^9}{\rho_e}(\text{cm})\,, \tag{4c}$$

and σ_i are the Pauli spin matrices. l_v is the oscillation length in vacuum and l is the refraction length in matter expressed in terms of G_F, the Fermi coupling constant of the weak interactions and $\rho_e=N_e(\text{cm}^{-3})/6\times 10^{23}$ is the electron density divided by Avogadro's number. (This value of l is obtained explicitly in the Appendix. It differs from that originally given by Wolfenstein[10] and used by Mikheyev and Smirnov,[9] by a factor $1/\sqrt{2}$ and in sign and agrees with the value in Refs. 12 and 13.) In a medium of constant density $n_{\nu_e}-n_{\nu_\mu}$ is independent of position and Eq. (4) can be solved by simple exponentiation. Utilizing the algebra of the Pauli spin matrices one can write the solution as

$$\begin{bmatrix}\nu_e\\ \nu_\mu\end{bmatrix}_x=\left[\cos(\pi x/l_m)+i\frac{l_m}{l_v}\sin(\pi x/l_m)(\alpha\sigma_1+\gamma\sigma_3)\right]\begin{bmatrix}\nu_e\\ \nu_\mu\end{bmatrix}_0 , \quad (5)$$

$$\begin{aligned}l_m&\equiv l_v/(\alpha^2+\gamma^2)^{1/2}\\&=l_v/[\sin^2 2\theta+(\cos 2\theta-l_v/l)^2]^{1/2} .\end{aligned} \quad (5a)$$

The probability that a pure ν_e state at $x=t=0$ appears later at $x=t$ as a ν_μ state can be read from Eq. (5):

$$\begin{aligned}P(\nu_e\to\nu_\mu,x)&=|\nu_\mu(x)|^2\\&=(l_m/l_v)^2\sin^2 2\theta\sin^2(\pi x/l_m) .\end{aligned} \quad (6)$$

Thus l_m is the oscillation length in matter. Note in particular that

$$P(\nu_e\to\nu_\mu,x)\to\begin{cases}\sin^2 2\theta\sin^2(\pi x/l_v) \text{ if } l_v/l\ll\cos 2\theta , & (7a)\\ (l/l_v)^2\sin^2 2\theta\sin^2(\pi x/l) \text{ if } l_v/l\gg 1 , & (7b)\\ \sin^2(\pi x\sin 2\theta/l_v) \text{ if } l_v/l=\cos 2\theta . & (7c)\end{cases}$$

Thus in a low-density medium where $l_v/l\ll\cos 2\theta$ [case (7a)] expression (6) reduces to the well-known expression for neutrino oscillations in vacuum,[1] while in a very dense medium, where $l_v/l\gg 1$ [case (7b)], the probability for oscillations is strongly suppressed, independent of the mixing angle. A complete flip of the lepton flavor of neutrinos, independent of the size of the mixing angle, takes place in a medium that satisfies the resonance condition $l=l_v/\cos 2\theta$ [case (7c)] at distances x_n which satisfy $x_n=(n+\frac{1}{2})l_v/\sin 2\theta$, $n=0,1,2,\ldots$. This is the resonance phenomenon that was discovered by Wolfenstein.[10]

In the general case when the density of the medium changes along the neutrino trajectory, Eq. (5) can be used to construct the solution to Eq. (4), as follows: one can divide the trajectory into segments where l is practically constant. In each individual segment $[x_{i-1},x_i]$ the propagation of the neutrinos is described by Eq. (5) with x replaced by $\Delta x_i=x_i-x_{i-1}$ and $l(x)$ replaced by $l_i\equiv l(x_{i-1}+\Delta x_i/2)$, i.e., if one rewrites Eq. (5) as

$$\begin{bmatrix}\nu_e\\ \nu_\mu\end{bmatrix}_{x_i}\simeq u_2(l_i,\Delta x_i)\begin{bmatrix}\nu_e\\ \nu_\mu\end{bmatrix}_{x_{i-1}} , \quad (8a)$$

then

$$\begin{bmatrix}\nu_e\\ \nu_\mu\end{bmatrix}_x\simeq\prod_i u_2(l_i,\Delta x_i)\begin{bmatrix}\nu_e\\ \nu_\mu\end{bmatrix}_0 , \quad (8b)$$

where $x=\sum_i\Delta x_i$. Solution (8) to Eq. (4) is an exact solution if l within each individual segment is a constant. It is, of course, an exact (formal) solution to Eq. (4) in the limit $\Delta x_i\to 0$.

Note, however, that "far" from the resonance, where $\gamma=l_v/l-\cos 2\theta\gg\cos 2\theta$, Eq. (4) reduces to

$$\frac{d}{dx}\begin{bmatrix}\nu_e\\ \nu_\mu\end{bmatrix}\simeq i\frac{\pi\gamma}{l_v}\sigma_3\begin{bmatrix}\nu_e\\ \nu_\mu\end{bmatrix} ,$$

whose solution is

$$\begin{aligned}\nu_e(x)&=\exp\left[i\pi\int\gamma\,dx/l_v\right]\nu_e(0) ,\\ \nu_\mu(x)&=\exp\left[-i\pi\int\gamma\,dx/l_v\right]\nu_\mu(0) ,\end{aligned}$$

while for $l_v/l\ll 1$ one obtains that $l_m\simeq l_v$ and Eq. (4) describes vacuum oscillations. Consequently in a medium with a density which changes with position the transition probability for $\nu_e\to\nu_\mu$ is negligible, if $\gamma\gg\sin 2\theta$, while it is given by expression (7a), if $l_v/l\ll 1$.

III. NUMERICAL SOLUTIONS

Although Eqs. (8) and (5) can be used to propagate neutrinos through matter, they require algebraic calculations with complex numbers. The use of complex numbers can be avoided, however, by transforming the two coupled equations (4), which are satisfied by the two complex functions $\nu_e(x)$ and $\nu_\mu(x)$, into a set of three coupled linear equations satisfied by the three real functions

$$\begin{aligned}A_1&=|\nu_e|^2-|\nu_\mu|^2 ,\\ A_2&=i(\nu_e^*\nu_\mu-\nu_e\nu_\mu^*) ,\\ A_3&=\nu_e^*\nu_\mu+\nu_e\nu_\mu^* .\end{aligned}$$

By multiplying Eq. (4) and its complex conjugate from the left by $(\nu_e,\nu_\mu)\sigma_i$ and $(\nu_e^*,\nu_\mu^*)\sigma_i$, respectively, and then by adding the two equations one obtains

$$\frac{d}{dx}\begin{bmatrix}A_1\\A_2\\A_3\end{bmatrix}=\frac{2\pi}{l_v}\begin{bmatrix}0&\alpha&0\\-\alpha&0&\gamma\\0&-\gamma&0\end{bmatrix}\begin{bmatrix}A_1\\A_2\\A_3\end{bmatrix} . \quad (9)$$

From the normalization condition $|\nu_e|^2+|\nu_\mu|^2=1$ one obtains that $A_1^2+A_2^2+A_3^2=1$ and that $|\nu_e|^2=(1+A_1)/2$ and $|\nu_\mu|^2=(1-A_1)/2$. In a medium of a constant density the solution of Eq. (9) can be written as $A(x)=u_3(\bar{l}_m,\bar{x})A(0)$, where the propagation matrix u_3 is given by

$$u_3(\bar{l}_m,\bar{x})=\bar{l}_m{}^2\begin{bmatrix} \gamma^2+\alpha^2\cos\bar{x} & \left[\dfrac{\alpha}{\bar{l}_m}\right]\sin\bar{x} & \alpha\gamma(1-\cos\bar{x}) \\ -\left[\dfrac{\alpha}{\bar{l}_m}\right]\sin\bar{x} & \bar{l}_m{}^{-2}\cos\bar{x} & +\left[\dfrac{\gamma}{\bar{l}_m}\right]\sin\bar{x} \\ +\alpha\gamma(1-\cos\bar{x}) & -\left[\dfrac{\gamma}{\bar{l}_m}\right]\sin\bar{x} & \alpha^2+\gamma^2\cos\bar{x} \end{bmatrix}, \tag{10}$$

where

$$\bar{l}_m \equiv l_m/l_v=\frac{1}{(\alpha^2+\gamma^2)^{1/2}} \tag{11}$$

and $\bar{x}\equiv 2\pi x/l_m$ [$\alpha=\sin 2\theta$ and $\gamma=(l_v/l-\cos 2\theta)$]. For the initial conditions $(\nu_e,\nu_\mu)_0=(1,0)$, i.e., $\mathbf{A}=(1,0,0)$, Eq. (10) yields the solutions

$$A_1=1-2(l_m/l_v)^2\sin^2 2\theta\sin^2(\pi x/l_m)\ , \tag{12a}$$

$$A_2=-(l_m/l_v)\sin 2\theta\sin(2\pi x/l_m)\ , \tag{12b}$$

$$A_3=-2(l_m/l_v)\sin 2\theta(\cos 2\theta-l_v/l)\sin^2(\pi x/l_m)\ . \tag{12c}$$

Equation (6) then follows from Eqs. (12) and $|\nu_\mu|^2=(1-A_1)/2$. If the density of the medium changes along the neutrino trajectory, one can divide the trajectory into segments where the density is approximately a constant and the propagation matrices are given by Eq. (10). Then the propagation matrix from 0 to x can be obtained by multiplying the propagation matrices in the individual segments

$$u_3(\bar{l}_m,\bar{x})=\prod_i u_3(l_m(\tilde{x}_i),\Delta\bar{x}_i)\ , \tag{13}$$

where $\Delta\bar{x}_i=\bar{x}_i-\bar{x}_{i-1}$, $2\tilde{x}_i=\bar{x}_i+\bar{x}_{i-1}$, and $\bar{x}=\sum\Delta\bar{x}_i$. Equation (13) is exact if either l is a constant in each individual segment, or $\Delta x_i\to 0$.

Equations (13) and (10) form the basis for our numerical solutions to the neutrino propagation equations (within the Sun, down to Earth and through Earth until reaching the underground neutrino detector). They have been used to test the analytic solutions that we have found for the neutrino propagation equations in the Sun, as described in Secs. IV and V.

IV. ANALYTIC SOLUTIONS FOR THE SUN

Let $\rho_e(r)$ denote the density of electrons in the Sun (divided by Avogadro's number) as a function of the distance r from the center of the Sun. The standard solar model yields a density distribution,[11] which decreases monotonically between $\rho(0)\simeq 115$ and $\rho(R_\odot)\sim 0$, where $R_\odot=6.96\times 10^{10}$ cm is the radius of the Sun. The scale height of the density distribution, defined as

$$H_\odot=-\rho_e/(d\rho_e/dr)\ , \tag{14}$$

decreases from its value $H_\odot\sim 0.66R_\odot$ near $r=0$ to become $H_\odot\sim 0.10R_\odot$ in the convective zone, $0.25\,R_\odot\lesssim r\lesssim R_\odot$.

Let us assume that a ν_e which is born in the core of the Sun passes through the resonance density $\rho_s=\rho_e(r_s)$ [for which $l(r_s)=l_v/\cos 2\theta$] on its way out from the Sun. Let χ denote the angle between the neutrino trajectory and the radius vector $\mathbf{r}_s$ (see Fig. 1). The effective scale height H, that the neutrino sees around r_s along its trajectory is thus given by

$$H=-\rho_e/(d\rho_e/dx)=H_\odot/\cos\chi\ . \tag{15}$$

The oscillation length in matter l_m, which is given by Eq. (5a) has a resonance shape around r_s. Its full width at half its height is given by $\Delta l/l_r=\tan 2\theta$. Since $l\sim\rho^{-1}$, the corresponding width in x space is given by

$$\frac{\Delta l}{l_r}=\frac{\Delta x}{l_r}\left[\frac{\Delta l}{\Delta x}\right]_{r_s}\simeq-\frac{\Delta x}{\rho_s}\left[\frac{d\rho}{dx}\right]_{x_r}=\frac{\Delta x}{H}=2\tan 2\theta\ , \tag{16}$$

i.e.,

$$\Delta x=2H\tan 2\theta\ . \tag{16a}$$

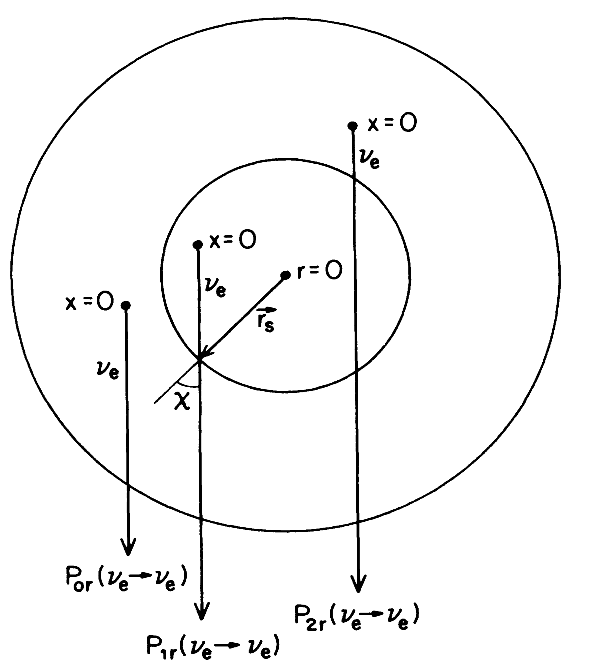

FIG. 1. Schematic description of the transition of solar neutrinos through a spherical resonance layer in the Sun.

Therefore we conclude that for small mixing angles for which $\Delta x \ll H$ the region $x_r - H \lesssim x \lesssim x_r + H$ is many times wider than the width of the resonance. Within this region the density may be well approximated by $\rho_e \simeq \rho_r[1+(x-x_r)/H]$ and Eq. (4) can be replaced there by

$$\frac{d}{d\bar{x}}\begin{bmatrix}\nu_e\\ \nu_\mu\end{bmatrix} = i(\alpha\sigma_1 - \beta\bar{x}\sigma_3)\begin{bmatrix}\nu_e\\ \nu_\mu\end{bmatrix}, \tag{17}$$

where

$$\bar{x} = \pi(x-x_r)/l_v, \quad \alpha = \sin 2\theta,$$

$$\beta = (l_v/\pi H)\cos 2\theta .$$

For small mixing angles the probability amplitude for the transition $\nu_e \to \nu_\mu$ can become significant only within this region: before this region, i.e., for $x \lesssim x_r - H$, the solution of Eq. (4) can be well approximated (see Sec. III) by $\nu_e(\bar{x}) = \exp(i\int \gamma d\bar{x})$, $\nu_\mu(\bar{x}) = 0$, i.e., the neutrino enters the resonance region as a pure ν_e state. Well beyond the resonance region ($x \gtrsim x_r + H$) the solution of Eq. (4) can be well approximated by the solution in a vacuum, which for small mixing angles yields a very small probability amplitude for the transition $\nu_e \to \nu_\mu$, $P(\nu_e \to \nu_\mu) \leq \sin^2 2\theta \ll 1$. Consequently the only significant transitions $\nu_e \to \nu_\mu$ can occur within the resonance region and can be calculated from the solution of Eq. (17) in the region $x_r - H < x < x_r + H$.

We shall now proceed to solve Eq. (17). By differentiating Eq. (17) we obtain

$$\frac{d^2}{d\bar{x}^2}\begin{bmatrix}\nu_e\\ \nu_\mu\end{bmatrix} = -[(\alpha^2 + i\beta\sigma_3) + \beta^2\bar{x}^2]\begin{bmatrix}\nu_e\\ \nu_\mu\end{bmatrix}, \tag{18}$$

i.e.,

$$\frac{d^2\nu_e}{d\xi^2} + (\tfrac{1}{4}\xi^2 - a)\nu_e = 0 , \tag{19}$$

where $\xi = \sqrt{2\beta}\,\bar{x}$ and $a = (-\alpha^2 - i\beta)/2\beta$. Equation (19) is the parabolic cylindrical equation whose solution is (see, for instance, Ref. 20, p. 686)

$$\nu_e(\xi) = A_1 y_1(-ia, \xi e^{i\pi/4}) + A_2 y_2(-ia, \xi e^{i\pi/4}) , \tag{20}$$

where A_1 and A_2 are constants, and y_1 and y_2 are, respectively, the even and the odd parabolic cylindrical functions:

$$y_1(-ia, \xi e^{i\pi/4}) = e^{-i\xi^2/4} M(i\alpha^2/4\beta, \tfrac{1}{2}, e^{i\pi/2}\xi^2/2) , \tag{21a}$$

$$y_2(-ia, \xi e^{i\pi/4}) = e^{i\pi/4}\xi e^{-i\xi^2/4} M(i\alpha^2/4\beta + \tfrac{1}{2}, \tfrac{3}{2}, e^{i\pi/2}\xi^2/2) . \tag{21b}$$

The functions $M(a,b,z)$ are Kummers functions. For $|z| \gg |a^2|, |b^2|$, they have the asymptotic form (see, Ref. 20, p. 508)

$$M(a,b,z) \simeq \Gamma(b)\left[\frac{e^{+i\pi a} z^{-a}}{\Gamma(b-a)} + \frac{e^z z^{a-b}}{\Gamma(a)}\right] . \tag{22}$$

Consequently for $|\xi| \gg \rho = \alpha^2/4\beta$,

$$y_1 \simeq \sqrt{\pi}\, e^{-\pi\rho/2}\left[\frac{e^{-i\phi}}{\Gamma(\frac{1}{2} - i\rho)} + \frac{\sqrt{2}\, e^{-i\pi/4} e^{+i\phi}}{|\xi|\,\Gamma(i\rho)}\right] = u_1 + v_1 , \tag{23a}$$

$$y_2 \simeq \sqrt{\pi}\, e^{-\pi\rho/2}\left[\frac{\xi e^{i\pi/2} e^{-i\phi}}{\sqrt{2}\,|\xi|\,\Gamma(1 - i\rho)} + \frac{e^{-i\pi/4} e^{+i\phi}}{\xi\Gamma(\frac{1}{2} + i\rho)}\right] = u_2 + v_2 , \tag{23b}$$

where $\phi = +i\xi^2/4 + i\rho\ln(\xi^2/2)$.

The initial conditions are $\nu_e(x=0) = \nu_e(\xi = -\xi_r = -\sqrt{2\beta}\pi x_r/l_v)$ and $\nu_\mu(-\xi_r) = 0$; and from Eq. (17) it follows that $(d\nu_e/d\xi)_{-\xi_r} = i\xi_r/2$. If we denote $\bar{u}_1 = u_1(-\xi_r)$, $\bar{v}_1 = v_1(-\xi_r)$, $\bar{u}_2 = u_2(-\xi_r)$, and $\bar{v}_2 = v_2(-\xi_r)$, then the initial conditions yield the relations

$$\begin{aligned} &\nu_e(x=0) = A_1(\bar{u}_1 + \bar{v}_1) + A_2(\bar{u}_2 + \bar{v}_2) = 1 , \\ &\frac{2}{i\xi_r}\left[\frac{d\nu_e}{d\xi}\right]_{\xi_r} \simeq A_1(\bar{u}_1 - \bar{v}_1) + A_2(\bar{u}_2 - \bar{v}_2) = 1 , \end{aligned} \tag{24}$$

whose solution is given by

$$\begin{aligned} &A_1 = \bar{v}_2/(\bar{u}_1\bar{v}_2 - \bar{u}_2\bar{v}_1) , \\ &A_2 = -\bar{v}_1/(\bar{u}_1\bar{v}_2 - \bar{u}_2\bar{v}_1) . \end{aligned} \tag{25}$$

Consider now the solution at the symmetric point ξ_r beyond the resonance point $\xi = 0$:

$$\nu_e(\xi_r) = A_1(u_1(\xi_r) + v_1(\xi_r)) + A_2(u_2(\xi_r) + v_2(\xi_r)) . \tag{26}$$

But u_1 and v_1 are symmetric functions of ξ while u_2 and v_2 are antisymmetric. Consequently

$$\nu_e(\xi_r) = A_1(\bar{u}_1 + \bar{v}_1) - A_2(\bar{u}_2 + \bar{v}_2) . \tag{27}$$

By substituting the explicit values of A_i, $\bar{u}_i$, and $\bar{v}_i$, $i = 1,2$, and by utilizing the relations

$$\Gamma(\tfrac{1}{2} - i\rho)\Gamma(\tfrac{1}{2} + i\rho) = \pi/\cosh(\pi\rho) , \tag{28a}$$

$$\Gamma(1 - i\rho) = -i\rho\Gamma(-i\rho) , \tag{28b}$$

$$\Gamma(-i\rho)\Gamma(i\rho) = \pi/\rho\sinh(\pi\rho) , \tag{28c}$$

one finally obtains

$$\nu_e(\xi_r) = e^{-2\pi\rho} + O(\sqrt{\rho}/\xi_r) , \tag{29}$$

$$p(\nu_e \to \nu_e, \xi_r) \simeq e^{-4\pi\rho} = e^{-\pi\alpha^2/\beta} . \tag{30}$$

If there is no significant change in this probability when the neutrino continues to propagate out of the Sun we arrive at *our main result*:

$$p_{1r}(\nu_e \to \nu_e) \sim e^{-(\pi^2 \sin^2 2\theta H)/(\cos 2\theta l_v)} . \tag{31}$$

where the subscript $1r$ indicates that the neutrino was born inside the spherical resonance layer (see Fig. 1). If the neutrino is born behind the resonance layer and it goes through it twice, then

$$p_{2r}(\nu_e \to \nu_e) = 1 - 2p_{1r} + 2p_{1r}^2 , \tag{32}$$

while for solar neutrinos that do not pass at all through the resonance layer $p_{0r}(\nu_e \to \nu_e) = 0$.

Note that the requirement $|\xi| \gtrsim \rho$ implies that Eq. (31) is a good approximation as long as

$$\tan^4 2\theta < \frac{32}{\pi} \frac{l_r}{H} . \tag{33}$$

Near the center of the Sun where $l_r \geq 10^7$ cm this implies the condition $\sin 2\theta \lesssim 0.3$, while it is less restrictive if the resonance layer is farther out.

Note also that Eq. (31) is valid only for neutrinos which are not born within the resonance. In particular, if $x_r = 0$, i.e., if the neutrino is born at the resonance point, then the solution to Eq. (19) is $\nu_e(\xi) = y_1(\xi)$. From the asymptotic form of y_1 it then follows that

$$p_{1r}(\nu_e \to \nu_e) = |y_1(|\xi| \gg \rho)|^2 = \frac{1 + e^{-2\pi\rho}}{2} . \tag{34}$$

In this paper we shall confine our attention to situations where $4\pi\rho \gtrsim 1$ at resonance, because only then the transition probabilities through the resonance, Eqs. (31) and (34), are significantly less than 1 and perhaps can account for the experimental observations on solar neutrinos. From the conditions $4\pi\rho = \pi^2 \sin^2 2\theta H / \cos 2\theta l_\nu \gtrsim 1$ and $l_\nu = l \cos 2\theta$ it then follows that

$$\tan^2 2\theta \gtrsim \begin{cases} 10^{-3}, & r_s \sim 0, \\ 10^{-4}, & r_s \gtrsim 0.1 R_\odot . \end{cases}$$

When x, the production point of the neutrino changes between $x \lesssim x_r - \Delta x/2$ and $x \gtrsim x_r + \Delta x/2$, $p(\nu_e \to \nu_e)$ changes between p_{1r} and 1, respectively. It assumes the value of Eq. (34) at $x = x_r$.

This behavior can be well described by the following expression:

$$p(\nu_e \to \nu_e) \simeq \begin{cases} p_{1r} = e^{-4\pi\rho} = \exp\left[-\frac{2.78 \times 10^9 \sin^2 2\theta}{\cos 2\theta} \left[\frac{H}{R_0} \right] \frac{\Delta m^2(\mathrm{eV}^2)}{E(\mathrm{MeV})} \right], & l(x) < \bar{l} , \\ \tilde{p}_{1r} = \dfrac{1}{1 + \exp\left[-\sqrt{2} \dfrac{\cos 2\theta - l_\nu / l}{\sin 2\theta} - 2\sqrt{p_{1r}} \right]}, & l(x) > \bar{l} , \end{cases} \tag{35}$$

where $l(x)$ is the refraction length of the Sun at the production point and $\bar{l}$ is defined $\tilde{p}_{1r}(l = \bar{l}) = p_{1r}$. Note that the arbitrary choice of the function $\tilde{p}_{1r}(l)$, which interpolates between p_{1r} and 1, has no practical importance because the fraction of neutrinos "born" in the resonance layer is relatively small. This is because the width of the resonance layer $\Delta x = 2H \tan 2\theta$, is much smaller than the width of the region in the Sun where the production of solar neutrinos takes place (if $\tan 2\theta \gg 1$). We selected that particular $\tilde{p}_{1r}(l)$ because $p_{1r}(l \gg l_r = l_\nu / \cos 2\theta) \to 1$ and $p_{1r}(l = l_r) \simeq (1 + e^{-2\pi\rho})/2$ [see Eq. (34)].

Equation (35) agrees well with numerical calculations (see Fig. 2).

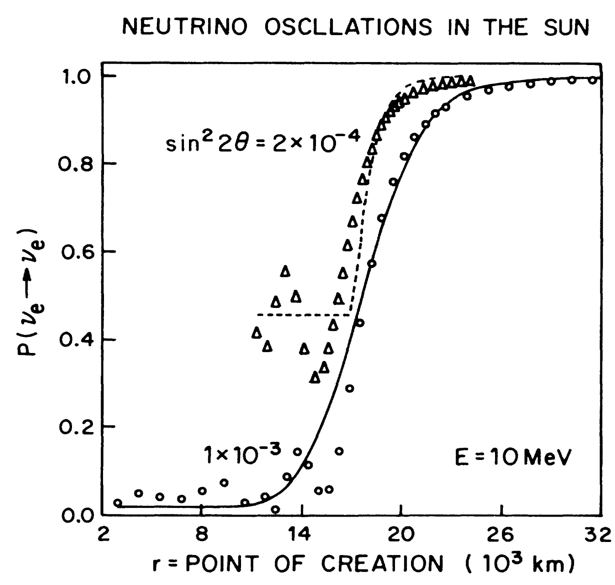

FIG. 2. $p(\nu_e \to \nu_e)$—the probability of an electron neutrino produced at a distance r from the center, and moving along a central trajectory, to emerge from the Sun, as an electron neutrino, as a function of r—the production point. The discrete marks were calculated numerically with Eq. (9) and a simple parametrization of the Sun's refraction length, specifically, $l(r) = l_C e^{r/H_0}$, where $l_C = 1.6 \times 10^7$ cm, $H_0 = 8 \times 10^9$ cm. The smooth line was obtained from the analytic expression (35). p was calculated for $\sin^2 2\theta = (2 \times 10^{-4}, 1 \times 10^{-3})$.

V. RESULTS

Equations (31) and (35) describe the transition probability of ν's through the resonance layer. However, these equations can be easily modified to include the effects of propagation before and after the resonance; at the end of Sec. II it was shown that neutrinos retain their flavor when they propagate in a medium with a density much higher than the resonance density, while they exhibit vacuumlike oscillations in regions with density below the resonance density. Consequently, (a) for neutrinos which do not cross the, resonance layers one obtains

$$\bar{p}_{0r}(\nu_e \to \nu_e) = 1 - \tfrac{1}{2} \sin^2 2\theta , \tag{36}$$

(b) for neutrinos which are born in the region surrounded by the resonance layer one obtains

$$\bar{p}_{1r}(\nu_e \to \nu_e) = \cos^2 2\theta p_{1r} + \tfrac{1}{2}\sin^2 2\theta \ , \tag{37}$$

and (c) for neutrinos which are born behind the resonance layer (and cross it twice) one obtains

$$\bar{p}_{2r}(\nu_e \to \nu_e) = 1 - \cos^2 2\theta \sin^2 2\theta + 2\cos^4 2\theta (p_{1r}{}^2 - p_{1r}) \ . \tag{38}$$

p_{1r} is given by Eq. (35) and the bars indicate averaging over detection position. This averaging has been invoked because of the change in the relative distance between the Sun and the underground detector (on Earth), due to the diurnal rotation of Earth and the eccentricity of its orbital motion around the Sun.

The closed-form expressions (35)—(38) for $p(\nu_e \to \nu_e)$ are the main results of our paper. We have compared these expressions with numerical solutions of the neutrino propagation equations in matter, which were obtained using the method described in Sec. III. We found excellent agreement between the closed-form expressions and the numerical results. This is demonstrated for the Sun in Figs. 3—5, where we compared our closed-form expressions with detailed numerical calculations and with those of Rosen and Gelb.

In Figs. 3(a) and 3(b) we compare the closed-form expressions (37) and (35), and the numerical results of Rosen and Gelb for $p(\nu_e \to \nu_e)$ at Earth as a function of $E/\Delta m^2$ for $\sin^2 2\theta = 0.01$ and $\sin^2 2\theta = 0.04$, respectively, assuming

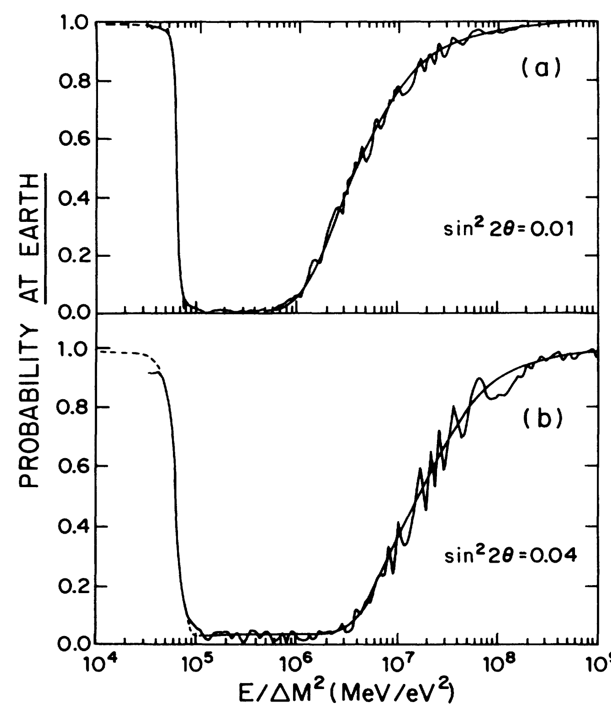

FIG. 3. Probability that a single electron neutrino, created at the center of the Sun, arrives at Earth versus $E/\Delta m^2$ for (a) $\sin^2 2\theta = 0.01$ and (b) $\sin^2 2\theta = 0.04$. The oscillating curves were calculated by Rosen and Gelb in Ref. 12. The smooth lines were obtained from the closed-form expressions (35)—(38).

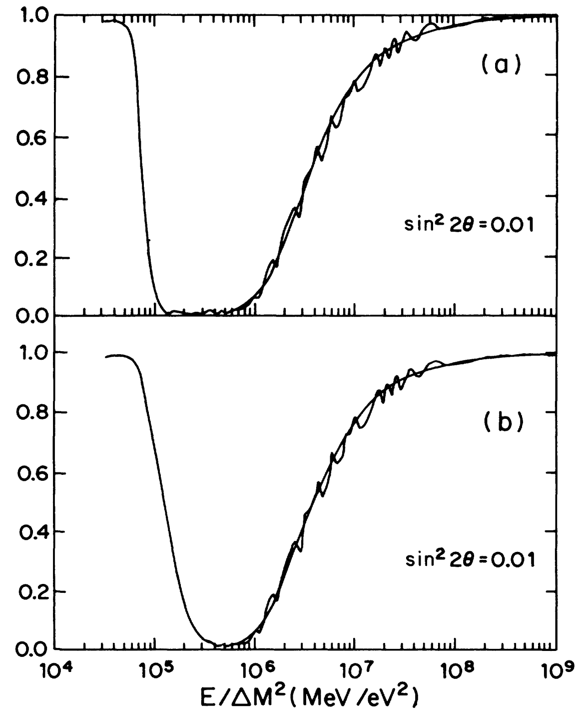

FIG. 4. Probability that a single electron neutrino created in the Sun (a) through ^{8}B decay and (b) through the pp reaction arrives at Earth versus $E/\Delta m^2$ for $\sin^2 2\theta = 0.01$. The oscillating curves were calculated by Rosen and Gelb in Ref. 12. The smooth lines were obtained from the closed-form expressions (35)—(38) as explained in the text.

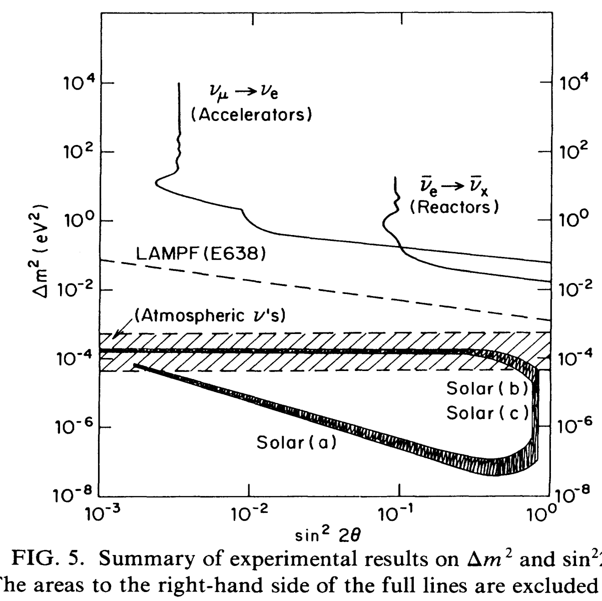

FIG. 5. Summary of experimental results on Δm^2 and $\sin^2 2\theta$. The areas to the right-hand side of the full lines are excluded by neutrino-oscillation experiments at accelerators and reactors. The area above the dashed line will be tested within a few years at LAMPF. The shaded areas can be tested by searching oscillations of atmospheric ν's with $0.1 \lesssim E_\nu \lesssim 1$ GeV. The black stripes indicate values that can solve the solar-neutrino problem, allowing only 1σ deviation in the reported theoretical and experimental values of ^{37}Ar production in the chlorine solar-neutrino experiment.

that all the solar ν_e's are produced at the center of the Sun. In the calculations we used the solar density distribution, which follows from the standard solar model and was tabulated by Bahcall *et al.*[11] and the expression for l that was used by Rosen and Gelb.[12] The results are sensitive only to the density distribution outside the solar core which can be well represented by an exponential density with $H_\odot \sim 0.1 R_\odot$. Note that according to Eqs. (34) and (35) $p(\nu_e \to \nu_e) \simeq \frac{1}{2}$ when the resonance condition

$$l\cos 2\theta = l_\upsilon = 2.47\times 10^2 \times E(\mathrm{MeV})/\Delta m^2(\mathrm{eV})^2 \ \mathrm{cm}$$

is satisfied at the center of the Sun. Rosen and Gelb used $l(0) \sim 1.59\times 10^7$ cm, which yields the value $E/\Delta m^2 \simeq 6\times 10^4\ \mathrm{MeV/eV^2}$, where $p(\nu_e \to \nu_e) = \frac{1}{2}$.

Figures 3(a) and 3(b) demonstrate excellent agreement between the closed-form expressions and the numerical results of Rosen and Gelb, if one uses the same solar model.

In Figs. 4(a) and 4(b) we compare our predictions, which follow from the closed-form expressions (35)—(38), and the numerical results of Rosen and Gelb for $p(\nu_e \to \nu_e)$ at Earth as a function of $E/\Delta m^2$ for $\sin^2 2\theta = 0.01$, for ^{8}B solar neutrinos, and for *pp* solar neutrinos, respectively. The spatial distributions of the production points of solar neutrinos were taken from the standard solar-model predictions that were tabulated by Bahcall *et al.*[11] Note that for $E/\Delta m^2 \geq 5\times 10^6\ \mathrm{MeV/eV^2}$ Figs. 3(a), 4(a), and 3(b) are practically identical. This is due to the fact that the resonance layer surrounds the whole neutrino production region for $E/\Delta m^2$ values beyond this value and all the neutrinos, which reach Earth, must cross the resonance layer, i.e., $p(\nu_e \to \nu_e) = \bar{p}_{1r}$. The production region of *pp* neutrinos extends up to[11] $r \equiv 0.5 R_\odot$, while the production region of ^{8}B neutrinos extends up to[11] $0.1 R_\odot$. For $r_s = 0.5 R_\odot$ the standard solar model yields[11] $\rho_s \sim 1.4$ and $l_s = l_r \simeq 1.2 \times 10^9$ cm. Consequently, the resonance condition $l_r \cos 2\theta = l_\upsilon = 2.47\times 10^2 E(\mathrm{MeV})/\Delta m^2(\mathrm{eV}^2)$ implies that all the neutrinos with $E/\Delta m \gtrsim 5\times 10^6$ cm, which are born at $r \leq 0.5 R_\odot$ cross a resonance layer at $r_s \geq 0.5 R_\odot$. For ^{8}B neutrinos the ν_e production is confined to $r \leq 0.12 R_\odot$. If $r_s \geq 0.12 R_\odot$, then $\rho_s \lesssim 59.5$ and $l_\upsilon > l_r \simeq 2.73\times 10^7$ which implies that Figs. 3(a) and 4(a) should coincide for $E/\Delta m^2 \gtrsim 1.2\times 10^5\ \mathrm{MeV/eV^2}$.

When $E/\Delta m^2$ decreases below $5\times 10^6\ \mathrm{MeV/eV^2}$, the resonance layer moves into the production region of the *pp* neutrinos. Since $p_{1r} \ll 1$ and $\sin^2 2\theta \ll 1$, it follows that both $\bar{p}_{2r} \simeq 1$ and $\bar{p}_{0r} \simeq 1$, i.e., all the neutrinos produced inside the resonance layer are transformed into ν_μ's, while those produced outside it survive as ν_e's. Consequently, in Fig. 3(b) the curve for $E/\Delta m^2 < 5\times 10^6\ \mathrm{MeV/eV^2}$ simply exhibits the fraction of *pp* neutrinos, which are produced beyond r_s that satisfies $l_\upsilon = 2.47\times 10^2 E(\mathrm{MeV})/\Delta m^2(\mathrm{eV}^2) = l(r_s)\cos 2\theta$ cm. Similarly, in Fig. 3(a) the curve for $E/\Delta m^2 \lesssim 1.2\times 10^5\ \mathrm{MeV/eV^2}$ describes the fraction of ^{8}B neutrinos that are produced beyond r_s that satisfies $l_\upsilon = l(r_s)\cos 2\theta$.

Figures 3(a), 3(b), 4(a), and 4(b) demonstrate that the closed-form expressions reproduce the values of $p(\nu_e \to \nu_e)$ at Earth obtained by numerical solution of the neutrino propagation equations in the Sun. Therefore, we shall use the closed-form expressions to evaluate the effects of neutrino oscillations in the Sun on the solar-neutrino experiments, and to determine the range of values of Δm^2 and $\sin^2 2\theta$ that can solve the solar-neutrino problem.

The rate of interaction of solar ν_e's in a detector on Earth is given by

$$R = N_a \int_{E_{\mathrm{th}}}^{E_{\max}} dE\, \sigma_{\nu_e}(E) p_{\nu_e}(E)(d\phi_\nu/dE) , \tag{39}$$

where N_a is the number of active atoms in the detector, σ_ν is their cross section for ν_e interaction, $d\phi_\nu/dE$ is the differential flux of solar neutrinos (all flavors) at Earth, and $p_{\nu_e}(E) = p(\nu_e \to \nu_e)$ at neutrino energy E. E_{th} is the energy threshold of the detector and $E_{\max}$ is the maximum energy of the solar neutrinos: $E_{\max} \simeq 14$ MeV. The predictions of the standard solar model[15] for the capture rate of solar ν_e's by the reaction $\nu_e + {}^{37}\mathrm{Cl} \to e^- + {}^{37}\mathrm{Ar}$ with $E_{\mathrm{th}} = 0.82$ MeV are summarized in Table I for $p_\nu = 1$. For a chlorine detector the theoretical prediction is[15]

$$(R/N_a)_{\mathrm{th}} = [5.8 \pm 0.73(1\sigma)]\times 10^{-36}\ \mathrm{sec}^{-1} \tag{40a}$$

while the experimental result of Davis *et al.*[5] is

$$(R/N_a)_{\exp} = [2.1 \pm 0.3(1\sigma)]\times 10^{-36}\ \mathrm{sec}^{-1} . \tag{40b}$$

The parameters Δm^2 and $\sin^2 2\theta$ which yield a reduction in the production rate of ^{37}Ar consistent with experiment can be found as follows.

In the standard solar model the production rate of ^{37}Ar is dominated by ^{8}B neutrinos [4.3 SNU (solar-neutrino unit) compared with 1.5 SNU from all other sources where 1 SNU $= 10^{-36}$ captures/^{37}Cl atom sec]. For ^{8}B neutrinos $E_{\max} d\phi_\nu/dE \sim x^2(1-x)^2$, where $x \equiv E_\nu/E_{\max}$ and $\sigma_\nu \sim x^{3.5}$. Therefore $\sigma_\nu d\phi_\nu/dx$ peaks around $x = 0.73$, i.e., around $E_\nu \sim 10$ MeV.

The transition probability of ^{8}B neutrinos through a resonance layer, as given by Eq. (31), is larger than that of all other solar neutrinos, by an enormous factor. This is because the effective energy of ^{8}B neutrinos, ~ 10 MeV, is much larger than the energies of the *pep*, ^{7}Be, and CNO neutrinos (see Table I). Consequently, there are three extreme possibilities to reduce the ^{37}Ar production rate to 2.1 SNU.

(a) All the production is due to ^{8}B neutrinos. This can happen only if two conditions are satisfied: (i) $p_{1r} = 0.5$ for $E_\nu \sim 10$ MeV *yielding* $\Delta m^2 \sin^2 2\theta/\cos 2\theta \sim 2.6\times 10^{-8}\ \mathrm{eV}^2$; (ii) $l_\upsilon(0.86\ \mathrm{MeV}) > l(0.12 R_\odot)\cos 2\theta$ *yielding* $\Delta m^2 \cos 2\theta \leq 7\times 10^{-6}\ \mathrm{eV}^2$. Condition (i) suppresses the ^{8}B contribution from the standard-model prediction of 4.3 SNU to the observed 2.1 SNU, while condition (ii) yields practically $p_{1r} \sim 0$ for the ^{7}Be, *pep*, and CNO neutrinos; i.e., it supresses completely their contribution.

(b) The resonance condition in the Sun is satisfied only for ^{8}B neutrinos; i.e., 1.5 SNU are due to ^{7}Be, *pep* and CNO neutrinos and the remaining 0.6 SNU are due to ^{8}B neutrinos. This happens if either the resonance layer surrounds the production region of ^{8}B neutrinos, i.e., $l_\upsilon(\sim 10\ \mathrm{MeV}) > l(0.12 R_\odot)$, and $p_{1r} = 0.6/4.3$ but $l_\upsilon(0.86\ \mathrm{MeV}) < l(r_s = 0)\cos 2\theta$, which yields (i) $\Delta m^2 \sin^2 2\theta/\cos\theta = 7\times 10^{-8}\ \mathrm{eV}^2$ *and* $1.5\times 10^{-5} < \Delta m^2 < 10^{-4}\ \mathrm{eV}^2$, or the resonance layer surrounds 86% ($= 1 - 0.6/4.3$) of the pro-

TABLE I. Neutrino fluxes and production rates predicted by the standard solar model (Ref. 15).

Reaction	Branching (%)	MaxE_ν (MeV)	Flux (10^{10} cm^{-2}sec^{-1})	^{37}Ar production rate (SNU)	^{71}Ge production rate (SNU)
		The pp chain			
$p+p\to D+e^{+}+\nu_e$	99.75	0.42	6.1	0	70.2
$p+e^{-}+p\to D+\nu_e$	0.25	1.44	1.5×10^{-2}	0.24	2.5
$D+p\to{}^{3}\mathrm{He}+\gamma$	100				
$^{3}\mathrm{He}+{}^{3}\mathrm{He}\to{}^{4}\mathrm{He}+2p$	86				
or					
$^{3}\mathrm{He}+{}^{4}\mathrm{He}\to{}^{7}\mathrm{Be}+\gamma$	14	0.86 (90%)	4.3×10^{-1}		
$^{7}\mathrm{Be}+e^{-}\to{}^{7}\mathrm{Li}+\nu_e$	99.89	0.38 (10%)		0.95	27.0
or					
$^{7}\mathrm{Be}+p\to{}^{8}\mathrm{B}+\gamma$	0.11				
$^{7}\mathrm{Li}+p\to2\,{}^{4}\mathrm{He}$	100				
$^{8}\mathrm{B}\to{}^{8}\mathrm{Be}^{*}+e^{+}+\nu_e$	100	14.06	4×10^{-4}	4.3	1.2
		The CNO cycle			
$^{12}\mathrm{C}+p\to{}^{13}\mathrm{N}+\gamma$					
$^{13}\mathrm{N}\to{}^{13}\mathrm{C}+e^{+}+\nu_e$		1.20	5×10^{-2}	0.08	2.6
$^{13}\mathrm{C}+p\to{}^{14}\mathrm{N}+\gamma$					
$^{14}\mathrm{N}+p\to{}^{15}\mathrm{O}+\gamma$					
$^{15}\mathrm{O}\to{}^{15}\mathrm{N}+e^{+}+\nu_e$		1.75	4×10^{-2}	0.24	3.5
$^{15}\mathrm{N}+p\to{}^{12}\mathrm{C}+{}^{14}\mathrm{He}$					
Total: $4p+2e^{-}\to{}^{4}\mathrm{He}+2\nu_e+26.73$ MeV		14.06	6.63	5.8	107.0

duction region of ^{8}B neutrinos and $p_{1r}\sim0$. Since 86% of the ^{8}B neutrinos are produced within $r\le0.075R_\odot$ and $H(0.075R_\odot)\sim0.2R_\odot$, it follows that (ii) $\Delta m^2\cos2\theta\sim1.2\times10^{-4}$ eV^2 and $10^{-3}<\sin^2 2\theta<0.3$.

(c) All the ν_e's convert in the Sun into ν_μ's ($p_{1r}\sim0$), but the ν_μ's oscillate in vacuum on their way to Earth and a fraction of about 2.1/5.8 ($=\frac{1}{2}\times\sin^2 2\theta$) reach the terrestrial detector as ν_e's, which yield $3\times10^{-8}<\Delta m^2<10^{-4}$ eV^2 *and* $\sin^2 2\theta\sim0.7$.

Solutions (a)—(c) define approximately a triangle in a Δm^2-$\sin^2 2\theta$ plane. If the 2.1 SNU is regarded as an upper bound then all values within the triangle can solve the solar-neutrino problem. Solutions (a)—(c) are indicated in Fig. 5 where we plotted the allowed values of Δm^2 and $\sin^2 2\theta$ which we obtained by taking the theoretical and experimental results at their face values ±1 standard deviation. The allowed regions become much wider if one allows larger errors in both the experimental and theoretical ^{37}Ar production rates. Our analytic solutions agree well with the solutions found by Rosen and Gelb through extensive numerical calculations.

The effects of the MSW solutions of the solar-neutrino problem on the proposed ^{71}Ga solar-neutrino experiments can also be easily calculated.

The main contribution to ^{71}Ge production in the ^{71}Ga experiments is due to pp and ^{7}Be neutrinos, as can be seen from Table I. Their maximum energies $E_{\max}$ are 0.42 and 0.87 MeV, respectively. If $\Delta m^2\ge2\times10^{-5}$ eV^2 these energies are below the lowest possible resonance energy in the Sun. Consequently, solutions (b) to the solar-neutrino problem do not affect the ^{71}Ga solar-neutrino experiments.

If, however, nature has selected Δm^2 and $\sin^2 2\theta$, which satisfy

$$\Delta m^2\sin^2 2\theta/\cos2\theta=2.6\times10^{-8}\ \mathrm{eV}^2$$

and $\Delta m^2\cos2\theta\lesssim10^{-5}$ eV^2, ($r_s\gtrsim0.12R_\odot$), then (i) the contribution of ^{7}Be neutrinos is reduced to ~0, since their production is inside the resonance layer and their transition probability through the resonance is $p_{1r}\sim0$, as follows from Eq. (35), and (ii) the production rate of ^{71}Ge in ^{71}Ga by pp neutrinos decreases fastly from 70.2 SNU for $\Delta m^2\ge10^{-5}$ eV^2 to practically zero for $\Delta m^2\le1.5\times10^{-6}$ eV^2. This is shown in Fig. 6, where we plotted both $p(\nu_i\to\nu_i)$ at Earth and the rate of production of ^{71}Ge in ^{71}Ga by pp neutrinos as function of Δm^2.

The behavior of $p(\nu_i\to\nu_i)$ shown in Fig. 6 can be easily understood: for $E_\nu=0.42$ MeV the resonance condition $l\cos2\theta=l_\nu$ and the solar density obtained from the standard solar model implies that the resonance position changes between $r_s=0$ for $\Delta m^2=10^{-5}$ eV^2 and $r_s=R_\odot/2$ for $\Delta m^2=10^{-6}$ eV^2. Consequently, for $\Delta m^2>10^{-5}$ eV^2, the energies of the pp neutrinos are below resonance, while for $\Delta m^2<10^{-6}$ eV^2 all the pp neutrinos are born inside the resonance layer and cross it on their way out of the Sun. From Eq. (35) it follows that the transition probability $p_{1r}(\nu_i\to\nu_i)$, through the resonance layer for pp neutrinos ($E_\nu\le0.42$ MeV) which satisfy the condition

$$\frac{\Delta m^2\sin^2 2\theta}{\cos2\theta}=2.6\times10^{-8}\ \mathrm{eV}^2\ ,$$

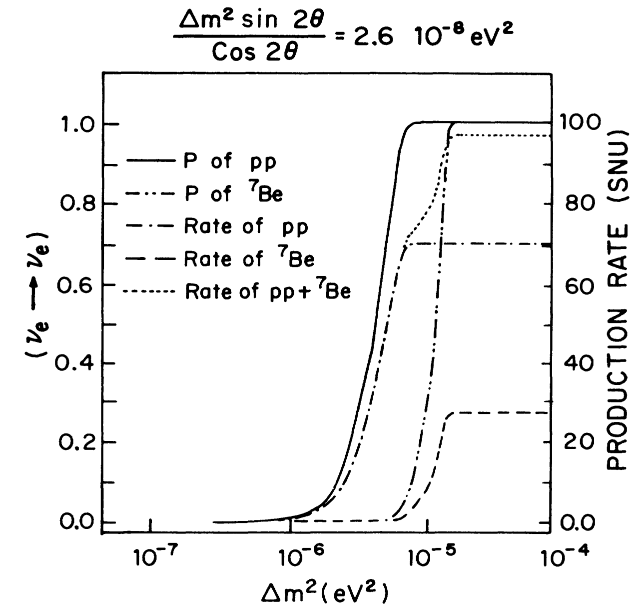

FIG. 6. Production rates of ^{71}Ge in ^{71}Ga due to *pp* and ^7Be neutrinos (right scale) and the probability of *pp* and ^7Be neutrinos to reach Earth as electron neutrinos versus Δm^2. In this figure we assumed solution (a): $\Delta m^2 \sin^2 2\theta / \cos 2\theta \approx 2.6 \times 10^{-8}$ eV^2.

is negligible.

Therefore if nature has selected neutrino masses and mixing angles that satisfy condition (a), then at Earth $p(\nu_i \to \nu_i) \simeq 1$ for *pp* neutrinos if $\Delta m^2 > 10^{-5}$ eV^2, while $p(\nu_i \to \nu_i) \simeq 0$ for *pp* neutrinos if $\Delta m^2 \lesssim 10^{-6}$ eV^2. This means that if solution (a) is responsible for the missing solar neutrinos in ^{37}Cl experiments, then the rate of production of ^{71}Ge in ^{71}Ga should be reduced from 107 SNU to a much smaller value if $\Delta m^2 \lesssim 2 \times 10^{-5}$ eV^2, depending on the value of Δm^2. In particular, the rate of production of ^{71}Ge in ^{71}Ga should decrease to ~ 0, if $\Delta m^2 \lesssim 10^{-6}$ eV^2. Note however, that our results are valid only when the Sun is above the horizon. As we shall see in the next section, oscillations of solar neutrinos in Earth modify the above predictions when the Sun is below the horizon (at night).

VI. NEUTRINO OSCILLATIONS IN EARTH

When the Sun is well above the horizon solar neutrinos travel only a short distance through Earth before reaching the underground solar-neutrino detector, but when the Sun approaches the horizon and goes below it the distance that solar neutrinos travel through Earth before reaching the underground detector becomes quite significant. For a detector at a depth d below the surface this distance is given by

$$L = [(R-d)^2 \cos^2 \mathcal{X} + d(2R-d)]^{1/2} - (R-d)\cos \mathcal{X} , \quad (41)$$

where $R = 6.37 \times 10^8$ cm is the radius of Earth and $\mathcal{X}$ is the zenith angle at the detector ($\mathcal{X}=0$ if the Sun is above the detector and $\mathcal{X}=\pi$ if the Sun is below the detector).

A flip of neutrino flavor can occur in Earth if two conditions are satisfied: (a) The neutrinos satisfy in Earth the resonance condition $l \cos 2\theta = l_v$, i.e., $l(\mathrm{cm}) = \sqrt{2}\pi / G_F n_e = 1.63 \times 10^9 / \rho_e = 2.47 \times 10^2 E(\mathrm{MeV}) / \Delta m^2 (\mathrm{eV}^2) \cos 2\theta$; (b) the width of the resonance is much smaller than both the scale height of the electron density near the resonance and the distance that the neutrino travels before the density suddenly changes.

If nature has selected $\Delta m^2 \simeq 1.2 \times 10^{-4}$ eV^2, then Earth is transparent to solar neutrinos. However, cosmic-ray-induced atmospheric neutrinos with 130 MeV $\lesssim E_\nu \lesssim$ 600 MeV can satisfy the resonance condition $l \cos 2\theta = l_v$ in Earth. Atmospheric neutrinos contain ν_e's and ν_μ's. Their ratio $R = N_{\nu_\mu} / N_{\nu_e}$ in the energy range 130 MeV $\lesssim E \lesssim$ 600 MeV depends only weakly on zenith angle ($R \sim 2.6$ for $\mathcal{X}=0$ and decreases to about $R \sim 2.0$ at $\mathcal{X} = \pi/2$) for down-going atomspheric neutrinos. For up-going neutrinos, $\mathcal{X} \gtrsim \pi/2$, their ratio can be related to their ratio when they enter Earth from the atmosphere at zenith angle $\pi - \mathcal{X}$ on the far side of Earth:

$$R \equiv (N_{\nu_\mu} / N_{\nu_e})_{\mathcal{X}} = \left[\frac{(1-p)R + p}{pR + (1-p)} \right]_{\pi - \mathcal{X}} , \quad (42)$$

where $p = p(\nu_e \to \nu_\mu)$ is the probability that a neutrino flips its lepton flavor when it crosses Earth from one side to the other at an angle $\pi - \mathcal{X}$. Since geomagnetic and solar wind effects *on the ratio* ν_μ / ν_e are quite negligible for $E_\nu \gtrsim 200$ MeV at most of the sites where the massive underground proton-decay detectors and neutrino telescopes are located,[16] Eq. (42) can be tested with experimental data obtained at the same site and the experimental results at different sites can be combined to increase statistics.[17]

In Fig. 7 we plotted R as a function of the zenith angle for atomspheric neutrinos with $E_\nu \sim 300$ MeV for representative values of $\sin^2 2\theta$ (4×10^{-2}, 10^{-2}, 4×10^{-3}, and 0). The ratio ν_μ / ν_e for down-going atmospheric neu-

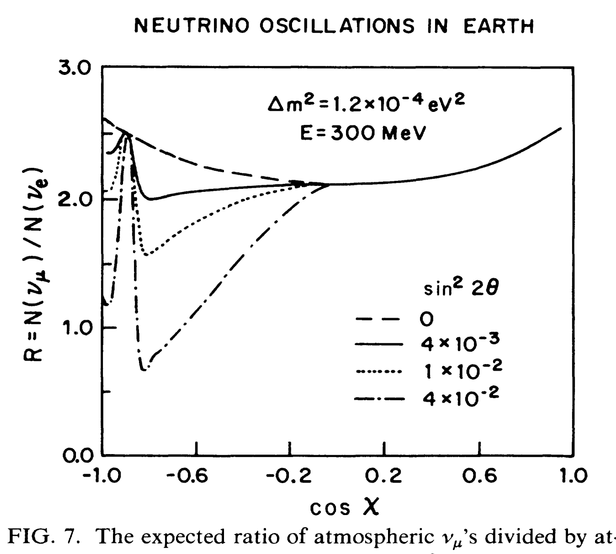

FIG. 7. The expected ratio of atmospheric ν_μ's divided by atmospheric ν_e's versus the zenith angle for $E_\nu = 0.3$ GeV, $\Delta m^2 \cos 2\theta = 1.23 \times 10^{-4}$ eV^2. The different lines are for the following values of $\sin^2 2\theta = (0, 4 \times 10^{-3}, 1 \times 10^{-2}, 4 \times 10^{-2})$. This ratio was calculated from expressions (9) and (42).

trinos was taken from the calculations of Dar,[16] which agree well both with experiments and with other independent calculations.[19]

$p(\nu_e \rightarrow \nu_\mu)$ for Earth as a function of the zenith angle was calculated by using Eq. (9) and the density distribution of Earth[18] shown in Fig. 11. As can be seen from Figs. 7 and 8 the effects of neutrino oscillations on R for $\Delta m^2 \simeq 1.2\times 10^{-4}$ eV^2 is quite significant for values of $\sin^2 2\theta$ which are not too small. Therefore the experimental data on the interactions of atmospheric neutrinos that have been accumulated in the massive underground proton-decay detectors (IMB, Kamiokande, Nusex, Soudan, and Frejus) should be carefully reanalyzed to see whether there is any confirmation to the MSW solution to the solar-neutrino problem. Note in particular that the energy range 200 MeV $\leq E_\nu \leq$ 400 MeV is exactly the energy range where most of the interactions of atomspheric neutrinos have been detected, i.e., $\sigma_\nu N_\nu$ for atmospheric neutrinos peaks within this energy range.

In Figs. 8, 9, and 10 we plotted R as a function of the energy, for atmospheric neutrinos with zenith angle $\mathcal{X}=180°$, 120°, and $0° < \mathcal{X} < 90°$, and various values of $\sin^2 2\theta$.

The electron density of Earth changes from about $\rho_e = n_e/N_A \sim 1.6$ near its surface to about $\rho_e \sim 6.3$ near its center.[18] Consequently, solar ν_e's with $0.24 \lesssim E_\nu \lesssim 14$ MeV may encounter a resonance density in Earth if $6\times 10^{-8} \leq \Delta m^2 \leq 1.4\times 10^{-5}$ eV^2.

The estimated effects of the MSW solution on the Cl and the Ga experiments neglected neutrino oscillations in Earth. At night solar neutrinos cross Earth before reaching the detector. Passage through Earth induces $\nu_e \leftrightarrow \nu_\mu$ transitions. Since the transition probability depends on the path length in Earth, i.e., on the position of the Sun relative to the detector, neutrino oscillations in Earth may induce both diurnal and seasonal modulations of the production rates in radiochemical detectors and changes in the rate and in the spectrum of recoiling electrons in electron-recoil detectors.

We have used Eq. (9) and the density distribution of Earth from Ref. 18 for calculating $P(\nu_e \leftrightarrow \nu_\mu)$, the probability of a neutrino flavor flip after crossing Earth. Our results are demonstrated in Fig. 12 where we plotted $P(\nu_e \leftrightarrow \nu_\mu)$ as a function of $E_\nu/\Delta m^2$, for $\sin^2 2\theta = 3\times 10^{-2}$ and various zenith angles of the incident ν_e's. As can be seen from Fig. 12 a significant probability of neutrino flavor flip develops for $\sin^2 2\theta \geq 10^{-2}$ and zenith angles z satisfying $\cos z \leq -0.25$, for neutrinos which satisfy the resonance condition in Earth. The electron density of Earth changes from $\rho_e \sim 1.3$ near its surface to about $\rho_e \sim 6.0$ near its center. Thus the resonance condition

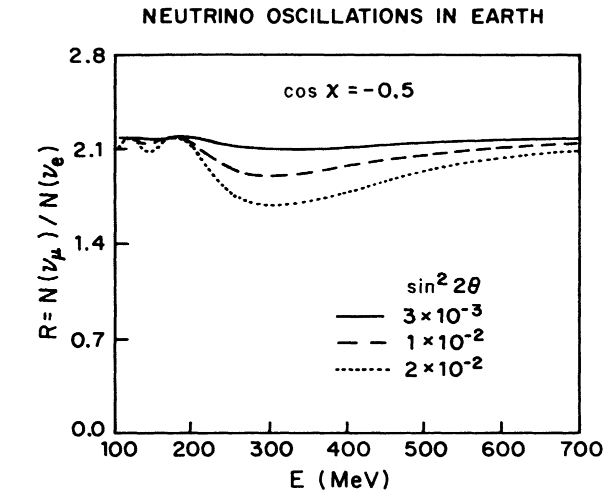

FIG. 9. The expected ratio of atmospheric ν_μ's divided by atmospheric ν_e's versus energy for zenith angle $\mathcal{X}=120°$. The different lines are for $\sin^2 2\theta = (3\times 10^{-3}, 1\times 10^{-2}, 2\times 10^{-2})$.

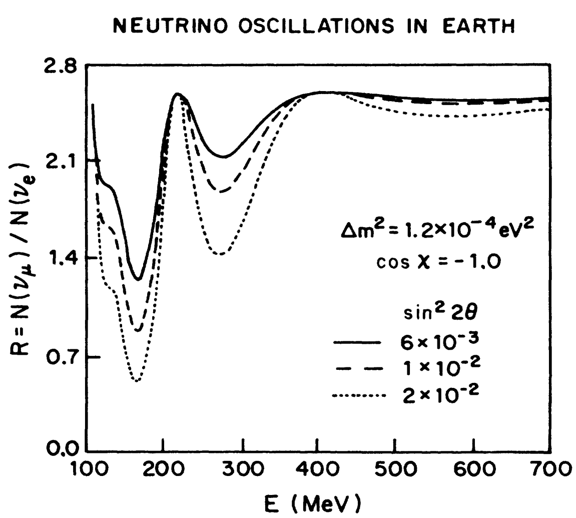

FIG. 8. The expected ratio of atmospheric ν_μ's divided by atmospheric ν_e's versus energy, for zenith angle $\mathcal{X}=180°$, $\Delta m^2 \cos 2\theta = 1.23\times 10^{-4}$ eV^2, and $\sin^2 2\theta = (6\times 10^{-3}, 1\times 10^{-2}, 2\times 10^{-2})$. The ratio was calculated with Eqs. (9) and (42).

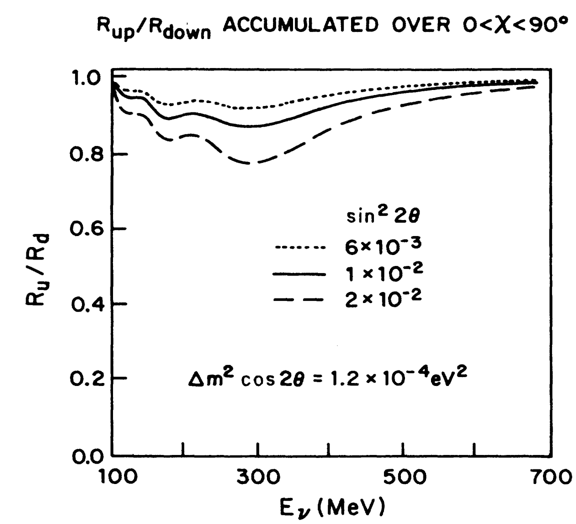

FIG. 10. The ratio $R = N(\nu_\mu)/N(\nu_e)$ for up-going atmospheric neutrinos accumulated over all zenith angles $0° \leq \mathcal{X} \leq 90°$ versus energy for $\sin^2 2\theta = (6\times 10^{-3}, 1\times 10^{-2}, 2\times 10^{-2})$ and energies $100 \leq E \leq 700$ MeV; $\Delta m^2 \cos 2\theta = 1.23\times 10^{-4}$ eV^2.

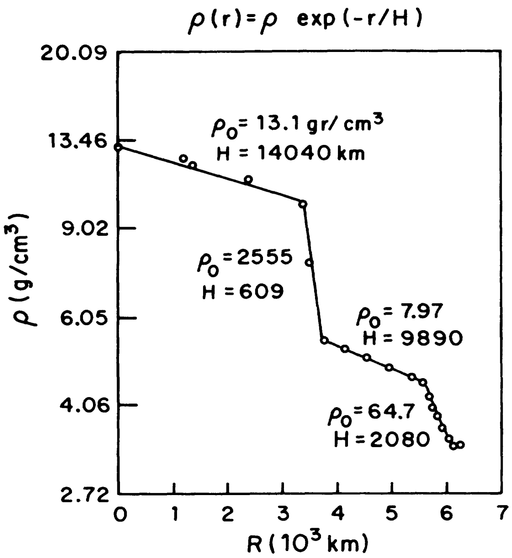

FIG. 11. Density distribution of Earth used in this paper. The squares are data taken from M.H.P. Bott [*The Interior of the Earth*, 2nd ed. (Arnold, London, 1982), p. 164], and were calculated in Ref. 18. The line is an interpolation fit, obtained by exponential functions, $\rho(r)=\rho_0\exp(-r/H)$ with different parameters (ρ_0,H) in different regions of the Earth interior. This fit was used in the numerical calculation of Figs. 7—10.

$l_v=l\cos2\theta$ in Earth is satisfied by neutrinos with $10^6\leq E/\Delta m^2\leq 5\times10^6$ MeV/eV^2.

The zenith angle of the Sun, z, as a function of time at a geographical latitude ϕ ($\phi\sim43°$N for Homestake, Mont Blanc, Frejus, Grand Sasso, and Baksan) is given by

$$\cos z=\sin\phi\sin\delta-\cos\phi\cos\delta\cos(2\pi h/23.934)\ , \quad (43)$$

where h is the day time (in hours), 23.934^h is the mean siderial day, and δ is the Sun's declination as a function of time. $\sin\delta\simeq-\sin(23.44°)\cos(2\pi d/365.242)$, where 23.44° is the angle at which the ecliptic is declined to the plane of the celestial equator, 365.242 is the length in days of a tropical year, and d is the time in the year (in days).

In Fig. 13 we plotted the yearly and seasonal time-averaged regeneration probabilities of solar neutrinos in Earth, that reach a terrestrial detector at night, at a geographical latitude 43°N, as a function of $E_v/\Delta m^2$, for $\sin^22\theta=0.1$ Figure 13 demonstrates that the regeneration probabilities in Earth can become quite large for mixing angles not too small. Consequently if solar neutrinos are converted in the Sun into ν_μ's then Earth may transform a large fraction of them, during nighttime, back into ν_c's and the day-night difference in the radiochemical detectors may be quite large (depending on the specific values of masses and mixing angles that nature has selected), as can be seen from Figs. 12—15. Unfortunately, the ^{37}Ar in the ^{37}Cl experiment was extracted after exposures between 35 and 80 days.[21] To reveal a day-night modulation one will have to extract continuously the Ar atoms produced in Cl (the Ge atoms produced in Ga) into separate day and night containers and count them separately, which apparently can be done with reasonable efficiencies.[22] However, a day-night difference, if it is sufficiently large should reveal itself also in a summer-winter difference. At 43°N the ratio between the average time that the Sun is below the horizon in the winter (October 1 through March 31) and in the summer (April 1 through September 30) is 1.40. Since the time-averaged probabilities in winter nights and in summer nights are approximately equal, therefore at Homestake the ratio between the numbers of Ar atoms produced in Cl by solar neutrinos during the winter and during the summer should be between 1 and 1.40 (1.40 if the MSW effect in the sun transforms all solar ν_c's into ν_μ's, less otherwise).

Indeed, the average production rate of Ar in Cl at Homestake was found to be 15% larger in the winter than in the summer (after correcting for seasonal changes in the distance to the Sun and excluding sessions which overlapped with large solar flares). However, the effect is of the same order as the statistical error (±20%) (Refs. 21 and 22).

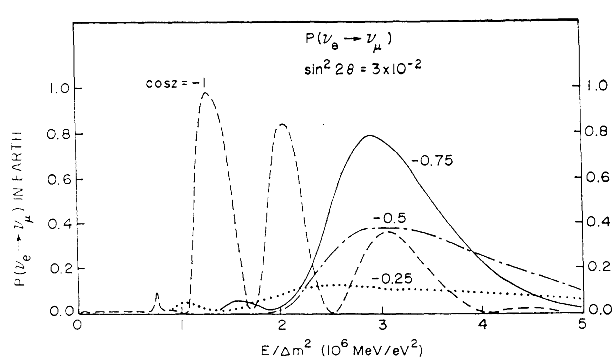

FIG. 12. The probability of neutrino flavor flip in Earth as a function of $E/\Delta m^2$ for $\sin^22\theta=3\times10^{-2}$, at various zenith angles.

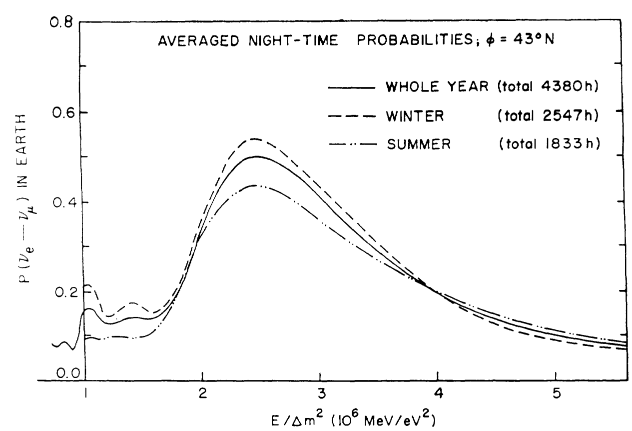

FIG. 13. The yearly and seasonal averaged probabilities of neutrino flavor flip in Earth for solar neutrinos that reach terrestrial detectors at a latitude 43°N during the night, as a function of $E_v/\Delta m^2$, for $\sin^22\theta=0.10$.

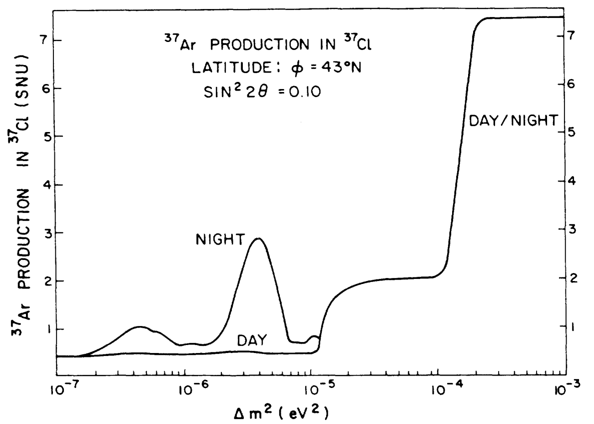

FIG. 14. The production rate of ^{37}Ar in ^{37}Cl at latitude 43°N as a function of Δm^2 during daytime and during nightime by solar neutrinos, for $\sin^2 2\theta = 0.10$.

VII. CONCLUSIONS

The values of neutrino masses and mixing angles, which are required by the Mikheyev-Smirnov-Wolfenstein solution to the solar-neutrino problem, can be found from analytic solutions to the neutrino propagation equations in the Sun. They practically coincide with those obtained through extensive numerical computations. They divide into three classes of oscillation parameters that can solve the solar-neutrino problem. The first class corresponds to the situation that only ^{8}B neutrinos encounter resonance denisties in the Sun and only 0.6 SNU of the 2.1 SNU observed production of ^{37}Ar in ^{37}Cl is due to ^{8}B neutrinos, while the rest 1.5 SNU is due to ^{7}Be, *pep*, and CNO neutrinos. The second class corresponds to the situation that practically all the ^{7}Be, *pep*, and CNO neutrinos and only a fraction of the ^{8}B neutrinos are transformed into ν_μ's in the Sun, and the observed ^{37}Ar production rate is due completely to the ^{8}B neutrinos which escaped the $\nu_e \to \nu_\mu$ transition. The third class corresponds to the situation that all the solar neutrinos are transformed in the Sun into ν_μ's, but vacuum oscillations on their way from the Sun to Earth transform about one-third of them back into ν_e's, which produce the ^{37}Ar atoms in ^{37}Cl.

If nature has selected the oscillation parameters to belong to the first class, then neutrino oscillations in the Sun have no effect on ^{71}Ge production in ^{71}Ga. However, these parameters yield sizable oscillations of atmospheric neutrinos in Earth, which can be detected by the massive deep-underground proton-decay detectors and neutrino telescopes.

If nature has selected the oscillation parameters to belong to either the second or third class, then the production of ^{71}Ge in ^{71}Ga by solar neutrinos is strongly reduced (less than 5 SNU during day time). These classes of oscillation parameters contain solutions that yield matter amplification of $\nu_e \leftrightarrow \nu_\mu$ transitions due to passage in Earth when the Sun is below the horizon. These transitions should show themselves as variations in production rates between day and night (perhaps possible by using more advanced detectors such as water Cherenkov detectors or heavy-water detectors) and between seasons (perhaps detectable by the radiochemical detectors).

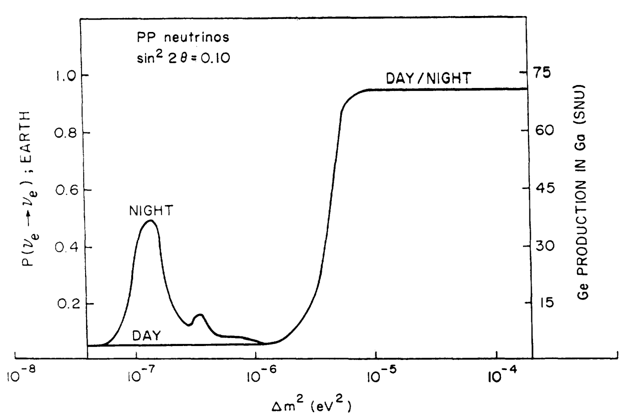

FIG. 15. The probability that *pp* neutrinos from the Sun reach a terrestrial detector at latitude 43°N as electron neutrinos, during daytime and during nighttime, as a function of Δm^2, for $\sin^2 2\theta = 0.10$, and the corresponding rate of ^{71}Ge production in ^{71}Ga.

ACKNOWLEDGMENTS

This work was supported in part by the Adler Foundation for Space Research and by the Technion Research Fund.

Note added. After completion of this work and during its proof for publication in this journal many authors have published relevant works. In particular, J. Bouchez *et al.*, Z. Phys. C **32**, 499 (1986), repeated the numerical calculations of Rosen and Gelb, included the effects of neutrino oscillations in Earth, and obtained similar results. W. C. Haxton [Phys. Rev. Lett. **57**, 1271 (1986)]; S. J. Parke [*ibid.* **57**, 1275 (1986)], and S. J. Parke and T. P. Walker [*ibid.* **57**, 2322 (1986)] found that the neutrino propagation equations in the Sun can be reduced to the quantum-mechanical problem of level crossing under the influence of an external linear field, which had been solved before by L. D. Landau [Phys. Z. Sowjetunion **2**, 46 (1932)] and C. Zener [Proc. R. Soc. London **A137**, 696 (1932)]. Their solution is identical to our analytic solution and indeed they showed that it leads to the three classes of solutions to the solar-neutrino problem which we found independently. E. W. Kolb *et al.* [Phys. Lett. **175B**, 478 (1986)] reproduced the "slab model" of Rosen and Gelb to explain the Rosen-Gelb solutions to the solar-neutrino problem. Finally, possible tests of the MSW solution to the solar-neutrino problem, using the matter amplification of oscillation of atmospheric neutrinos and of solar neutrinos in Earth, were discussed also by J. LoSecco [Phys. Rev. Lett. **57**, 652 (1986)], by E. Carlson [Phys. Rev. D **34**, 1454 (1986)], by A. J. Baltz and J. Weneser [Phys. Rev. D **35**, 528 (1987)], and by M. Cribier *et al.* [Phys. Lett. **182B**, 89 (1986)], who arrived at similar conclusions to ours.

APPENDIX

In the standard theory of the electroweak interactions the amplitude for $\nu_e e \rightarrow \nu_e e$ scattering via W exchange is given by

$$M = \frac{G_F}{\sqrt{2}} \frac{M_W{}^2}{M_W{}^2 - k^2} \bar{\nu}(q_2)\gamma^\mu(1-\gamma_5)e(p_1)\bar{e}(p_2)$$

$$\times \gamma_\mu(1-\gamma_5)\nu(q_1) ,$$

where G_F is the Fermi coupling constant, M_W is the mass of the W boson, q_1 and p_1 are the initial four-momenta of the ν_e and the electron, respectively, q_2 and p_2 are their final momenta, respectively, and $k = p_1 - q_2 = p_2 - q_1$ is the four-momenta transferred by the W.

The c.m. amplitudes for forward scattering of electrons with helicities $\pm\frac{1}{2}$ are obtained by performing the spinor and matrix multiplication and are given by

$$f(0) = \left[\frac{d\sigma}{d\Omega}(\theta=0) \right]^{1/2} = \frac{M}{\sqrt{64\pi^2 s}} ,$$

$$M[\nu_e(-)+e(-)\rightarrow\nu_e(-)+e(-)] = 8\sqrt{2}\, G_F k_\nu \sqrt{s} ,$$

all other combinations give $M=0$ (s is the c.m. energy squared and k_ν the c.m. momentum of the neutrino), i.e., $f_-(0) = (\sqrt{2} G_F k_\nu / \pi) f_+(0) = 0$ where the subscripts $+/-$ indicate $\pm\frac{1}{2}$ initial (and final) electron helicities. Consequently

$$\Delta n = n(\nu_e) - n(\nu_\mu)$$

$$= \frac{2\pi}{k_\nu{}^2}[f_-(0)\times N_e(-\tfrac{1}{2}) + f_+(0)\times N_e(+\tfrac{1}{2})]$$

$$= \frac{2}{k^2} f_-(0) \frac{N_e}{2} ,$$

i.e.,

$$l = \frac{2\pi}{k_\nu \Delta n} = \frac{\sqrt{2}\,\pi}{G_F N_e} = \frac{1.63\times 10^9}{\rho_e}(\text{cm}) .$$

[1] S. M. Bilenky and B. Pontecorvo, Phys. Rep. **41C**, 276 (1978).

[2] B. Pontecorvo, Zh. Eksp. Teor. Fiz. **53**, 1717 (1967) [Sov. Phys. JETP **26**, 984 (1968)]; 33, 549 (1957) [**6**, 429 (1958)]; **34**, 247 (1958) [**7**, 172 (1958)].

[3] J. N. Bahcall and R. Davis, Science **191**, 264 (1976).

[4] H. Fritzsch and P. Minkowski, Phys. Lett. **62B**, 72 (1976); J. N. Bahcall *et al.*, Phys. Rev. Lett. **40**, 1351 (1978).

[5] J. K. Rowley, B. T. Cleveland, and R. Davis, Jr., in *Solar Neutrinos and Neutrino Astronomy, proceedings of the Conference, Lead, South Dakota, 1984*, edited by M. L. Cherry, K. Lande, and W. A. Fowler (AIP Conf. Proc. No. 126) (AIP, New York, 1985).

[6] S. Nussinov, Phys. Lett. **63B**, 201 (1976).

[7] For a recent review see, for instance, J. Wotschak, in *Multiparticle Dynamics 1985*, proceedings of the XVIth International Symposium, Kiryat Anavim, Israel, 1985, edited by J. Greenhaus (World Scientific, Singapore, 1986), pp. 3–15.

[8] Oscillations of cosmic-ray neutrinos with oscillation length of the order of the diameter of Earth were searched, e.g., by J. M. LoSecco *et al.*, Phys. Rev. Lett. **54**, 229 (1985).

[9] S. P. Mikheyev and A. Yu. Smirnov, Nuovo Cimento **9C**, 17 (1986).

[10] L. Wolfenstein, Phys. Rev. D **17**, 2369 (1978); **20**, 2634 (1979).

[11] J. N. Bahcall *et al.*, Rev. Mod. Phys. **54**, 767 (1982).

[12] S. P. Rosen, Los Alamos Report No. LA-UR-86-1233, 1986 (unpublished); S. P. Rosen and J. M. Gelb, Phys. Rev. D **34**, 969 (1986).

[13] H. A. Bethe, Phys. Rev. Lett. **56**, 1305 (1986).

[14] P. K. Kabir, *The CP Puzzle* (Academic, New York, 1968).

[15] J. N. Bahcall *et al.*, Astrophys. J. **292**, L79 (1985).

[16] A. Dar, Phys. Rev. Lett. **51**, 227 (1983), and references therein.

[17] A. Dar, A. Mann, and Y. Melina (unpublished).

[18] A. N. Dziewonski and K. L. Anderson, Preliminary Reference Earth Model Phys. Earth Planet Interiors **25**, 297 (1981).

[19] T. K. Gaisser *et al.*, Phys. Rev. Lett. **51**, 223 (1983), and references therein.

[20] M. Abramowitz and I. A. Stegun, *Handbook of Mathematical Functions* (Dover, New York, 1965).

[21] R. Davis, Jr., Proceedings of the 7th Workshop on Grand Unification, ICOBAN 86, 1986, Toyama, Japan (unpublished).

[22] R. Davis, Jr. (private communication).